MINERALOGICAL MAGAZINE

VOLUME 54 NUMBER 376 SEPTEMBER 1990

Chemical variation in micas from the Cairngorm pluton, Scotland

T. N. HARRISON*

Department of Geology and Mineralogy, Marischal College, University of Aberdeen, Aberdeen AB9 1AS, Scotland

Abstract

Electron microprobe analyses of micas from the Cairngorm pluton in the Eastern Grampian Highlands of Scotland show extensive compositional variation in biotite, despite a lack of chemical variation in the host granite. Biotite has high Fe/(Fe + Mg) (0.6–0.85) and Al^{vi} (0.6–2.1 a.f.u.), and enrichment trends in these two parameters are attributable to the Al-Tschermak and dioctahedral–trioctahedral substitutions, the latter becoming dominant with increasing Al^{vi} content. Ti content is low (0.2–0.4 a.f.u.), and is largely controlled by a Tschermak-type substitution. Biotite is also unusually rich in Mn (up to 2.57 wt.% MnO), which increases with both Al^{vi} and Fe/(Fe+Mg). F contents generally range between 0.55 and 2.05 wt.% All compositional variation in biotite can be attributed to the extensive development of a fluid phase during the late-magmatic and subsolidus evolution of the pluton. The presence of an abundant fluid phase has resulted in the alteration of biotite to muscovite, which has occurred in response to de-stabilization of the biotite as octahedral R^{2+} cations are lost in favour of Al. Extreme build-up of this fluid phase has resulted in the crystallization of muscovite as a late, interstitial primary phase. Both primary and replacive muscovite have Fe/(Fe+Mg) > 0.50, 15–36 mol.% celadonite and <1 mol.% paragonite.

KEYWORDS: biotite, muscovite, chemical variation, Cairngorm pluton, Scotland.

Cation substitution in biotite

CATION substitution in biotite has been extensively reviewed by Foster (1960), Hazen and Wones (1972), Dymek (1983) and Hewitt and Abrecht (1986), whilst Thompson (1982) and Labotka (1983) have used linear algebraic methods to study compositional variation in either biotite (Labotka) or silicates generally (Thompson). In this paper, biotite is discussed in terms of its 'traditional' end-members annite, phlogopite, siderophyllite, and eastonite which, despite their apparent simplicity, are as open to ambiguity as more complex multi-end-member studies of complete biotite analyses (Hewitt and Abrecht, 1986). Furthermore, the study of biotite compositional variation using natural end-members is fraught with difficulty when using microprobe data, for which no Fe^{3+}, Li or H_2O analyses are available. In view of the extensive literature on the subject, it is proposed to present only an outline of the main substitution mechanisms governing tetrahedral and octahedral compositional changes so as to establish a framework for discussion of data in subsequent sections. Only variations in Al, Ti, Fe, Mg and Mn are considered.

The dominant mechanism for Al-enrichment in biotites is through the Al-Tschermak substitution

* Present address: 53½ Powis Place, Aberdeen AB2 3TT.

$$(R^{2+})^{vi} + Si^{iv} = Al^{iv} + Al^{vi}, \quad (1)$$

relating the end-members phlogopite, annite, eastonite, and siderophyllite. Foster (1960) has suggested that Al^{vi}-enrichment can also be accomplished by a coupled dioctahedral–trioctahedral substitution

$$3(R^{2+})^{vi} = 2Al^{vi} + (\ )^{vi}, \quad (2)$$

linking muscovite and biotite. The creation of an octahedral vacancy for Al^{vi} maintains the charge balance in the octahedral sheet as substitution (2) tends to impart a positive charge to the sheet. Hewitt and Wones (1975) have shown that the length of the K–O bond in the interlayer sheet has a fundamental influence upon the Al content of synthetic biotite. Increasing Al content enlarges the octahedral sheet and requires rotation of the tetrahedral sheet in order to accommodate the structural misfit. However, the tetrahedral rotation angle is constrained by the length of the K–O bond, thereby limiting the amount of Al^{vi} that can be accommodated.

Fe^{2+}, Mg, or Mn substitutions may be achieved by either sample proxying or by more complex substitutions such as (1), (2), the Ferri-Tschermak substitution

$$(R^{2+})^{vi} + Si^{iv} = (Fe^{3+})^{vi} + Al^{vi} \quad (3)$$

or through the substitution

$$(Fe^{3+})^{vi} + (Fe^{2+})^{vi} = Mg^{vi} + Al^{vi}. \quad (4)$$

Fe^{3+} may also enter tetrahedral coordination if there is insufficient Al^{iv} to fill the site, although this situation is not realised in aluminous bulk compositions.

Barrière and Cotten (1979) have suggested that the substitution

$$4Fe^{2+} + 4(OH)^- = 4Fe^{3+} + 4O^{2-} + 2H_2 \quad (5)$$

becomes important during the oxidation of a biotite-bearing granitic magma.

Ti substitution in biotites is complicated by its charge and small cationic radius (0.61 Å), compared with Fe^{2+} (0.78 Å) and Mg (0.72 Å) (Whittaker and Muntus, 1970). Ti may enter biotite by several substitution mechanisms:

$$3(R^{2+})^{vi} + Si^{iv} = Ti^{vi} + 2Al^{vi} \quad (6)$$

$$Al^{vi} + Si^{iv} = Ti^{vi} + Al^{iv} \quad (7)$$

$$2(R^{2+})^{vi} = Ti^{vi} + (\ )^{vi} \quad (8)$$

$$2Al^{vi} = Ti^{vi} + (R^{2+})^{vi}. \quad (9)$$

Cation substitution in muscovite

The muscovite group has three end-members:

Muscovite (*sensu stricto*)	$KAl_2(Si_3Al)O_{10}(OH)_2$
Celadonite	$K(AlR^{2+,3+,4+})Si_4O_{10}(OH)_2$
Paragonite	$NaAl_2(Si_3Al)O_{10}(OH)_2$.

Continuous solid solution occurs between the muscovite and celadonite end-members, and this group is often referred to as the phengite group. However, the term 'phengite' should ideally be restricted to those compositions containing 40 to 90 mol.% celadonite. Muscovites are herein considered in terms of the end-members muscovite (*sensu stricto*), celadonite, and paragonite. Compositional variations in this group are dominated by Tschermak-type substitutions such as (1), (3), and (6), although Fe^{3+} can also substitute simply for Al^{vi}. In addition to these substitutions, compositional variation in phengites can be achieved through the substitution

$$2Al^{iv} + Si^{iv} = 2Al^{vi} + 2(R^{2+})^{vi}. \quad (10)$$

Ti substitution in natural muscovite has been reviewed extensively by Monier and Robert (1986), who show that the dominant mechanism is Ti-Tschermak substitution.

Interlayer substitution in muscovite is limited, as there is no complete solid-solution series with paragonite. Compositional variation may occur in response to direct substitution of K for Na or through the illite substitution

$$K^{xii} + Al^{iv} = (\ )^{xii} + Si^{iv}. \quad (11)$$

Celadonite muscovites and biotites are linked through substitution (2), although Monier (1987) has shown that increased Li substitution reduces the miscibility gap between the two micas.

Geological setting of the Cairngorm pluton

The Cairngorm pluton is the largest in a series of post-tectonic, broadly calc-alkaline granites that were emplaced into the Scottish Caledonian metamorphic belt between 435 and 390 Ma, some 55–25 Ma after the peak of orogeny. The pluton (Fig. 1) is a composite body of coarse, pink porphyritic and non-porphyritic biotite adamellite (corresponding to monzogranite of Streckeisen, 1976) which have gradational internal contacts. Numerous small flat-lying bodies of porphyritic aplogranite (or microgranite), associated with pegmatites and aplites, are developed, and these are frequently drusy (Harrison, 1987*a*).

The chemistry of all units of the pluton is moderately peraluminous, with molar $Al_2O_3/(CaO+Na_2O+K_2O)$ between 1.10 and 1.30, 1.5–4.0% normative corundum, and SiO_2 content between 74 and 77 wt.%. The chemistry is typical of a minimum melt granite, with CaO <1.5 wt.%,

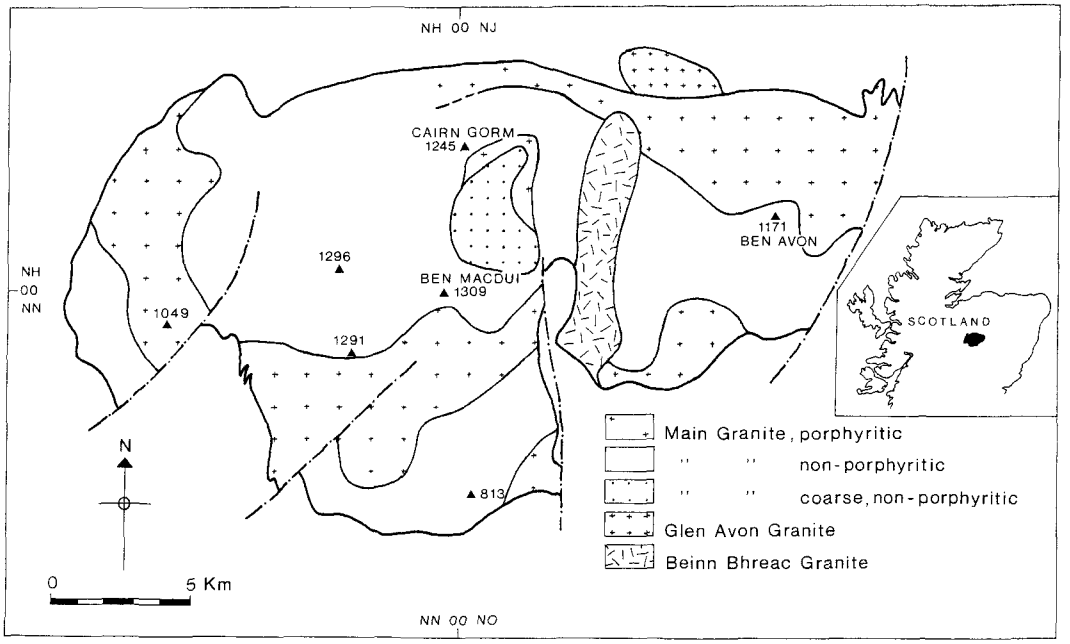

FIG. 1. Simplified geological map of the Cairngorm pluton, modified after Harrison (1987*a*). Minor granites are omitted for clarity. Figures at the map margin refer to the British National system. Heights are in metres.

MgO <1.0 wt.%, and P_2O_5 <0.05 wt.% (Harrison, 1987*b*). There is no systematic difference in chemistry between the various units and no discernible differentiation sequence within the pluton.

All members of the pluton are petrographically monotonous, with equal amounts of brown quartz, pink plagioclase (An_{10-20}), and pink K-feldspar composing 95–98% of the mode. Biotite is the only mafic silicate present, although there is local muscovite. The accessory mineral suite is varied, with ubiquitous zircon, apatite, Fe–Ti oxides, and widespread monazite. Minor Fe–Mn garnet is found at some marginal localities (Harrison, 1988).

The pluton was emplaced at a high crustal level (4–6 km), and its emplacement was probably controlled by the formation of a large tensional cavity in response to locking on large, coeval NE–SW strike-slip faults. Emplacement itself was accomplished by rapid and massive-scale stoping of large blocks of the predominantly psammitic envelope rocks (Harrison, 1987*a*).

It should be noted that much of the area lies within a National Nature Reserve or is designated a Site of Special Scientific Interest, and as such a permit is required from the Nature Conservancy Council for scientific research within these areas.

Biotite

Petrography

Biotite is the only mafic silicate in the Cairngorm pluton, and seldom exceeds 5% of themode. It has generally crystallized later than plagioclase (from which it is largely absent as inclusions) and before K-feldspar and quartz, both of which enclose biotite. Biotite is anhedral to subhedral and usually shows the pleochroic schemes $\beta = \gamma$ = olive-green to pale straw-yellow, α = olive-green, and $\beta = \gamma$ = greenish-brown to deep yellow-brown, α = deep olive-green. However, on rare occasions the biotite shows $\beta = \gamma$ = foxy red-brown to straw-yellow, α = foxy red-brown. This red-brown biotite generally coexists with Mn-rich magmatic garnet and may reflect the buffering effect of the garnet on f_{O_2} during biotite crystallization (Harrison, 1988), this biotite having crystallized under more reducing conditions than the olive-green variety.

Biotite often develops finger-like secondary overgrowths extending into adjacent K-feldspar or plagioclase, and may also form a symplectic intergrowth with quartz and magnetite replacing K-feldspar. These biotite overgrowths are in optical continuity with the primary crystal and are compositionally identical. Biotite is often extens-

ively altered to either brown thuringitic chlorite or to muscovite. Both have replaced biotite as lenses along the cleavage, but muscovite has also pervasively replaced biotite grains and forms as narrow rims at biotite/K-feldspar interfaces.

In contrast to the largely subhedral biotite in the granite, biotite from aplites and pegmatites often shows extreme elongation ratios along the X crystallographic axis, ranging between 1:16 and 1:37. This texture may have developed in response to the quenching of undercooled residual granitic magma during emplacement. The biotite morphology may also be dictated to some extent by the concentration of water at the melt/crystal interface during crystallization (cf. Fenn, 1986).

Analytical techniques

The pluton has been sampled on an approximate 1 km grid, and biotite has been analysed from 51 samples. Two or three grains per sample were analysed (two points per grain), and representative analyses of single points are presented in Table 1. The difference in composition between each analysis on a single grain is <3 wt.%of each element, except for Na where the difference is <5 wt.%.

All mineral analyses were made using a Cambridge Instruments Geoscan IV microprobe and Link Systems EDS 290 system. Acceleration voltage was 15 kV, with 200 s livetime count times. ZAF 4 FLS correction factors were applied. F analyses were made using a wavelength-dispersive Cambridge Instruments Microscan microprobe under similar operating conditions.

Mineral chemistry

Al substitution. The Cairngorm biotites are particularly rich in Al^{vi} in comparison with biotites from many other granites (e.g. de Albuquerque, 1973; Barrière and Cotten, 1979; Czamanske *et al.*, 1981; Dodge *et al.*, 1969), ranging from 0.1 to 2.1 a.f.u. (atoms per formula unit, on an anhydrous basis of 22 oxygens; Table 1). The distribution of Al^{vi} is controlled largely by the Al-Tschermak substitution (1) and, with increasing Al content, (2). Tschermak-type substitutions are also important. The effect of substitution (2) on the composition of the Cairngorm biotite is shown in Fig. 2, the data defining the approximate trend of $(\ )^{vi} = 2\ Al^{vi}$. There would appear to be two parallel trends, labelled A and B. Trend A is defined by the 'typical' biotites in the pluton and shows a rather restricted spread of both Al^{vi} and $(\ )^{vi}$. Biotites from trend B have slightly higher $(\ )^{vi}$ relative to Al^{vi} than those from trend A and show a much greater compositional range. The majority of trend B biotites coexist with either late muscovite or extensively sericitized plagioclase and their separate trend reflects the increased importance of a dioctahedral component, as introduced by substitution (2). It is this relationship that compositionally links biotite and late muscovite.

Fe and Mg substitution. Al plays a dominant role in both the nature of the Fe and Mg substitutions and in the absolute amount of both cations in the biotite. Hewitt and Wones (1975) have shown that the substitution of Al^{vi} for $(Fe,Mg)^{vi}$ will decrease the size of the octahedral sheet, whereas substitution of Fe for Mg will increase its size. In theory, therefore, the two substitutions could balance each other out. This is clearly not the case in the Cairngorm pluton because biotite contains more Al than the octahedral sheet can easily accommodate, and there is no relationship between Fe (as total iron, FeO) and Mg.

There is, however, an excellent correlation between Al^{vi} and Fe/(Fe+Mg) (Fig. 3).When combined with the conclusions drawn from Fig. 2, this shows that the proxying of an octahedral vacancy for R^{2+} cations through substitution (2) becomes increasingly dominant over the Al-Tschermak substitution with increasing Al content. Therefore, the most aluminous biotites also have the lowest R^{2+} contents, helping to explain the lack of any relationship between Fe and Mg.

Ti substitution. The Ti contents of the Cairngorm biotites are comparatively low in comparison with biotites from other published analyses of granitic biotites, ranging from 0.1 to 0.5 a.f.u. Ti only shows a moderate correlation with Fe/(Fe+Mg), although the correlation with both Al^{vi} (Fig. 4) and $(\ )^{vi}$ is excellent, indicating the importance of the Ti-Tschermak substitution (6). There is also a positive correlation between high Fe/(Fe+Mg) and low Ti, contrary to the experimental work of Robert (1976) whose results actually show that the octahedral substitution $2R^{2+} = Ti$ is maximized when Mg is much greater than Fe.

The relatively low Ti contents in the Cairngorm biotites may reflect the composition of the source area, which is envisaged to be granulite of granitic or granodioritic composition (Harrison and Hutchinson, 1987). There is no petrographic or geochemical evidence to suggest Ti depletion of the melt (as monitored through the low Ti contents of the biotite) through widespread fractionation of Ti-rich phases such as titanite or ilmenomagnetite.

Mn substitution. The Cairngorm biotites are unusually Mn-rich, with up to 2.57 wt.% MnO. Mn enters biotite through simple substitution for

Table 1. *Composition of biotites from the Cairngorm pluton.*

SAMPLE	CG1	CG13	CG41	CG43	CG47	CG50	CG62	CG75	CG79	CG83	CG85	CG88	CG97	CG98	CG106	CG112	CG121	CG129	CG131	CG138	CG141	CG144	CG150
SiO_2	37.60	37.70	37.03	38.16	42.24	36.94	39.22	35.83	38.79	36.09	36.02	35.47	35.27	35.66	36.71	37.13	37.46	35.92	36.79	36.64	36.43	38.43	36.55
TiO_2	2.53	2.14	3.86	2.58	0.85	2.39	2.36	3.14	2.15	2.52	2.24	2.66	2.40	2.71	2.87	2.90	2.63	2.29	2.08	2.07	2.39	1.67	2.22
Al_2O_3	16.48	18.73	13.55	18.62	22.17	18.42	19.80	17.68	20.11	19.20	18.50	17.56	19.56	19.39	19.33	16.78	14.21	19.45	19.16	17.91	18.77	20.92	18.82
FeO	24.56	22.04	25.76	23.01	17.01	23.69	21.10	23.42	20.24	22.92	24.62	24.92	24.75	24.03	24.10	23.99	24.12	23.34	22.93	21.39	23.46	19.51	21.89
MnO	0.97	1.07	0.73	1.58	2.56	1.27	1.53	0.72	1.53	1.88	1.84	1.32	0.88	1.29	1.53	1.24	0.56	1.06	1.67	0.94	1.60	2.21	1.48
MgO	5.05	4.81	7.25	2.55	0.90	3.28	2.08	6.15	3.06	3.03	3.35	2.98	3.08	3.21	3.24	4.19	6.77	4.13	2.75	4.87	3.50	0.54	3.20
Na_2O	0.26	0.26	0.21	0.33	0.31	0.21	0.46	0.59	0.54	0.49	0.40	0.39	0.31	0.52	0.56	0.47	0.33	0.51	0.21	0.24	0.12	0.15	0.65
K_2O	9.82	9.89	9.89	9.79	10.15	9.69	9.32	9.98	9.68	9.70	9.91	9.57	9.28	9.37	9.69	9.31	9.10	9.66	9.51	9.60	9.67	9.68	9.30
Total	96.70	96.51	98.28	96.62	96.19	96.16	95.87	97.51	96.10	95.83	96.88	94.84	96.65	96.18	98.03	96.01	95.18	96.36	95.10	93.66	95.94	93.11	94.11
Structural formulae calculated on an anhydrous basis of 22 cations																							
Si	5.797	5.723	5.675	5.817	6.208	5.697	5.885	5.466	5.839	5.590	5.577	5.504	5.532	5.511	5.568	5.742	5.841	5.526	5.714	5.742	5.639	5.966	5.714
Al	2.203	2.277	2.325	2.183	1.792	2.303	2.115	2.534	2.161	2.410	2.423	2.396	2.468	2.398	2.432	2.258	2.159	2.474	2.286	2.258	2.361	2.034	2.286
Al	0.667	1.073	0.124	1.162	2.049	1.047	1.387	0.644	1.407	1.095	0.953	0.875	0.984	1.043	1.025	0.800	0.451	1.053	1.220	1.050	1.063	1.794	1.183
Ti	0.293	0.244	0.447	0.296	0.094	0.277	0.266	0.360	0.243	0.293	0.261	0.316	0.325	0.315	0.327	0.337	0.309	0.265	0.243	0.244	0.278	0.194	0.262
Fe	3.160	2.798	3.301	2.934	2.091	3.091	2.648	2.989	2.549	2.969	3.187	3.293	3.212	3.105	3.057	3.102	3.145	3.003	2.979	2.804	3.037	2.533	2.863
Mn	0.126	0.138	0.094	0.203	0.318	0.166	0.194	0.093	0.195	0.247	0.241	0.177	0.128	0.169	0.197	0.162	0.074	0.138	0.220	0.124	0.209	0.290	0.196
Mg	1.159	1.089	1.657	0.597	0.196	0.754	0.465	1.399	0.679	0.700	0.774	0.702	0.767	0.739	0.733	0.965	1.572	0.947	0.637	1.138	0.807	0.124	0.745
Total	5.405	5.432	5.623	5.192	4.793	5.335	4.960	5.485	5.073	5.304	5.416	5.363	5.416	5.371	5.339	5.367	5.551	5.406	5.299	5.360	5.394	4.935	5.429
Na	0.076	0.075	0.062	0.098	0.088	0.061	0.133	0.175	0.158	0.146	0.120	0.113	0.100	0.157	0.164	0.140	0.098	0.151	0.128	0.073	0.036	0.046	0.196
K	1.928	1.891	1.934	1.905	1.902	1.906	1.785	1.943	1.859	1.916	1.957	1.929	1.868	1.848	1.874	1.837	1.809	1.897	1.885	1.919	1.909	1.918	1.856
Fe/(Fe+Mg)	0.732	0.719	0.666	0.835	0.914	0.804	0.850	0.681	0.789	0.809	0.804	0.824	0.807	0.808	0.806	0.763	0.667	0.760	0.824	0.711	0.790	0.953	0.794
Al/(Al+Si)	0.331	0.369	0.301	0.365	0.332	0.370	0.373	0.368	0.379	0.385	0.377	0.368	0.384	0.391	0.383	0.348	0.309	0.390	0.380	0.366	0.378	0.391	0.378

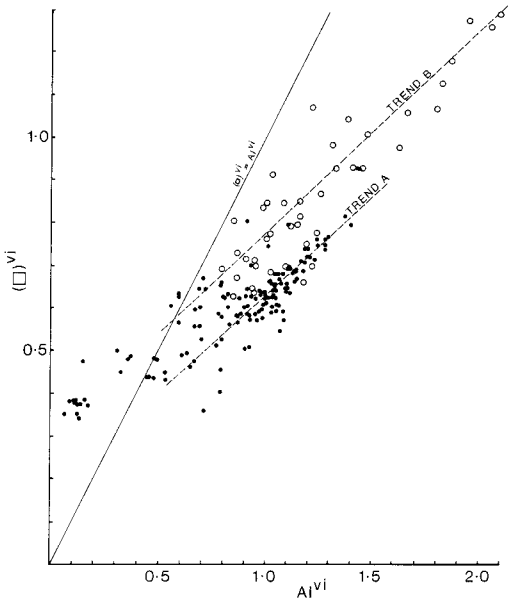

FIG. 2. ( )^{vi} *vs.* Al^{vi} in Cairngorm biotite. Open circles indicate biotite coexisting with either muscovite or extensively sericitised feldspar.

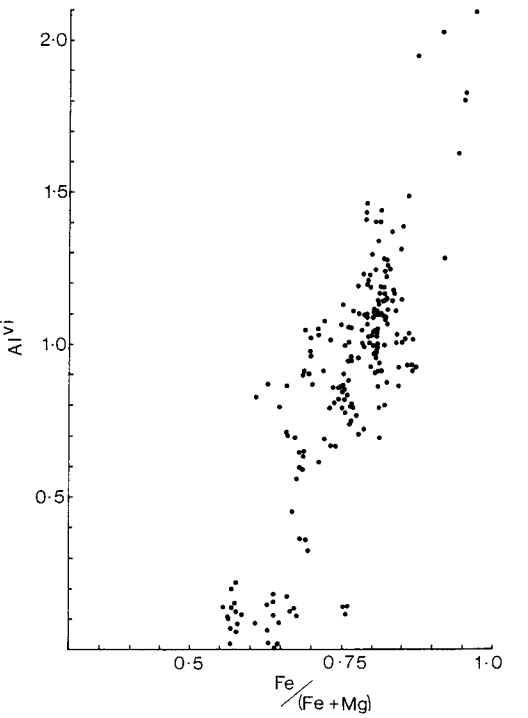

FIG. 3. Al^{vi} *vs.* Fe/(Fe + Mg) in Cairngorm biotite.

Fe, and Mn increases concomitantly with Fe/(Fe+Mg) (Fig. 5).This trend steepens significantly with increasing Fe/(Fe+Mg) which suggests than Mn may also be involved in a Tschermak-type substitution at high Fe/(Fe+Mg). The cause of the Mn-enrichment may be due to the absence of any significant amounts of pyroxene or amphibole fractionation during the early stages of the magma's evolution (Harrison, 1988), since both have high K_{Mn} in silicic liquids (Mahood and Hildreth, 1983).

The most Mn-rich biotites also coexist with muscovite, and both Mn and Al^{vi} increase concomitantly. This suggests that the evolution of the fluid phase exerted a significant control over the Mn content of the micas during the late evolution of the pluton.

Halogens. F has been analysed in biotite from 33 samples, and ranges between 0.55 and 2.05 wt.% (not shown in Table 1). Whilst it is not proposed to deal with the possibly complex effect of F on cation substitution in biotite (I. Parsons, R. Mason, and S. Becker, in prep.), it is pertinent to note that F contents increase in a linear fashion with increasing ( )^{vi}. F does not show correlations with any other parameter. Cl contents are uniformly low (*c.* 0.05 wt.%).

Li has not been determined, although zinnwaldite is found in several of the pegmatitic bodies associated with porphyritic aplogranites (Harrison, 1987*b*). This suggests that Li may also be an important component of biotite in some circumstances (e.g. CG47, Table 1), and may result in an overestimation of octahedral vacancies in these analyses.

Muscovite

Petrography

Muscovite is widespread but never common in the Cairngorm pluton and never accounts for more than 5% of the mode. It occurs as two distinct textural types—'primary looking' and secondary. 'Primary looking' muscovite takes the form of large interstitial poikilitic plates up to 3 mm across. Textural evidence shows these too have been the last mineral to form, and despite failure to satisfy the main criterion for primary muscovite (namely a euhedral habit; Miller *et al.*, 1981), they do not appear to have replaced any other phases, and probably formed under late magmatic or immediately subsolidus conditions.

Secondary muscovite has several habits. It has replaced biotite, either as lenses along the cleavage or pervasively across the grain, and muscovite

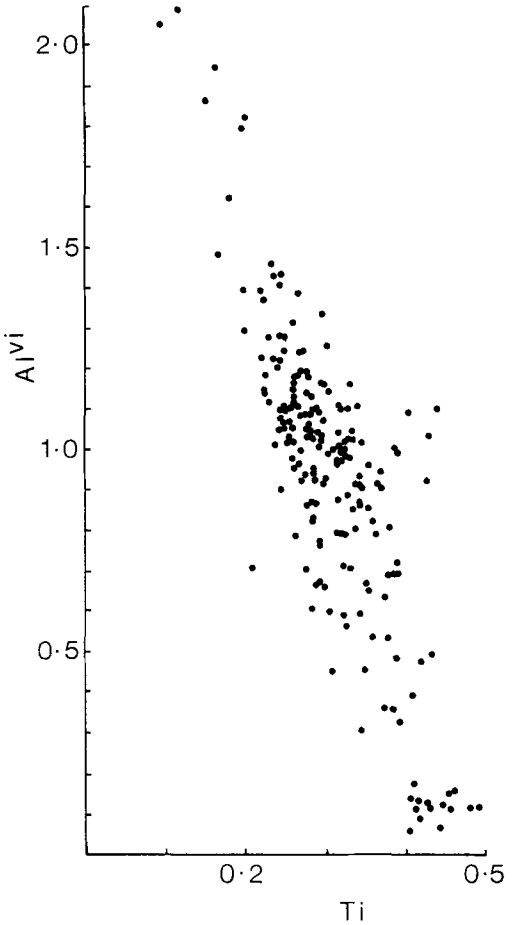

FIG. 4. Al^{vi} *vs.* Ti in Cairngorm biotite.

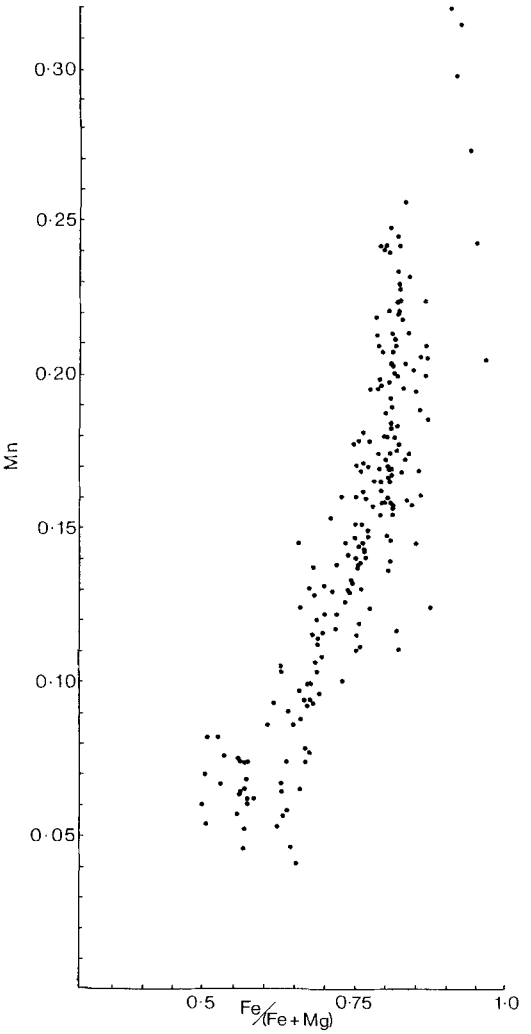

FIG. 5. Mn *vs.* Fe/(Fe + Mg) in Cairngorm biotite.

grains with biotite cores are seen. In the latter, the interface between the muscovite rims and biotite cores is always extremely sharp, even at the limits of conventional optical microscopic resolution. This textural variety of muscovite is distinguished from the 'primary looking' muscovite by the absence of poikilitic texture and its association with biotite 'relics'. Secondary muscovite also occurs as a by-product of the sericitization reaction of feldspars and is distinguished by its smaller grain size.

Mineral chemistry

Analytical techniques are the same as those used for biotite, and representative analyses of Cairngorm muscovite from 22 samples are presented in Table 2. They contain between 15 and 36 mol.% celadonite with the data plotting close to the ideal distribution defined by the Al-Tschermak substitution (1). These compositions lie within the stability field of aluminous phengites with $Fe/(Fe+Mg) = 0.50$ at $P_{H_2O} = 2$ kbar (Velde, 1965), although the temperature range for the reaction of biotite to phengite is large (300–500°C) and decreases with increasing celadonite content. It is clear, however, that these temperatures are significantly subsolidus.

Fig. 6*a* shows that the muscovite compositions deviate significantly from the Al-Tschermak substitution when defined in terms of Si and Al(tot), and this deviation is taken to indicate the presence of a ferrimuscovite component. Leroy and Cathelineau (1982) have attempted to quantify Fe^{3+} contents of microprobe-analysed muscovites

Table 2. *Composition of muscovites from the Cairngorm pluton.*

SAMPLE	CG13	CG47	CG57	CG61	CG79	CG82	CG83	CG85	CG88	CG131	CG141	CG143	CG144
SiO_2	47.36	46.62	45.76	45.85	46.36	45.95	45.66	46.09	46.04	45.94	47.05	46.97	46.59
TiO_2	0.46	0.38	0.55	0.59	0.48	0.23	0.53	0.82	0.21	0.13	0.68	0.54	0.46
Al_2O_3	28.33	27.22	26.45	28.44	28.01	28.71	28.60	30.68	29.23	28.20	31.34	27.80	27.73
FeO	5.77	9.26	8.22	5.64	7.49	6.50	6.45	5.35	5.61	7.82	4.91	6.49	9.64
MnO	0.19	1.16	0.61	0.17	0.58	0.29	0.36	0.09	0.08	0.66	0.12	0.40	1.05
MgO	1.79	0.65	2.19	1.18	1.71	1.17	1.59	1.37	1.16	0.69	1.56	1.60	0.61
Na_2O	0.31	0.36	0.79	0.45	0.51	0.43	0.73	0.87	0.27	0.44	0.43	0.37	0.50
K_2O	10.80	11.17	10.44	10.16	10.54	10.87	10.57	11.04	10.95	10.66	10.89	10.89	10.68
Total	95.01	96.82	95.01	92.48	95.68	94.15	94.49	96.31	93.55	94.54	96.98	95.06	97.26
Structural formulae calculated on an anhydrous basis of 22 cations													
Si	6.491	6.440	6.354	6.447	6.385	6.369	6.344	6.243	6.408	6.422	6.318	6.411	6.405
Al	1.509	1.560	1.646	1.553	1.615	1.631	1.656	1.757	1.592	1.578	1.682	1.589	1.593
Al	3.276	2.872	2.683	3.161	2.932	3.059	3.028	3.141	3.203	3.070	3.279	2.980	2.899
Ti	0.047	0.039	0.057	0.062	0.049	0.024	0.055	0.083	0.022	0.014	0.068	0.056	0.046
Fe	0.698	1.070	0.954	0.663	0.863	0.754	0.750	0.606	0.653	0.914	0.551	0.810	1.108
Mn	0.048	0.136	0.071	0.020	0.068	0.034	0.042	0.028	0.010	0.078	0.014	0.047	0.122
Mg	0.392	0.134	0.454	0.247	0.352	0.241	0.329	0.277	0.241	0.145	0.231	0.332	0.125
Na	0.066	0.097	0.213	0.123	0.137	0.114	0.196	0.229	0.073	0.119	0.113	0.101	0.132
K	1.945	1.968	1.849	1.822	1.852	1.922	1.873	1.907	1.945	1.901	1.866	1.938	1.873

using a similar relationship, and using their method the Cairngorm muscovites contain 0.4–0.6 Fe^{3+} a.f.u.

There is an incomplete solid-solution series between muscovite (*sensu stricto*) and paragonite. The Cairngorm muscovites lie very close to the muscovite end of the muscovite–paragonite compositional join, with <1 mol.% paragonite component. Na and K do not show any regular distribution (Fig. 6*b*), which may be due to non-stoichiometry of the interlayer site in response to substitution (11). However, the data scatter about the line Na + K = 2.0, suggesting that the interlayer site occupancy is essentially complete.

The amount of solid solution between the various end-members may be used as a broad indicator of the muscovite paragenesis. The work of Velde (1972) has shown that celadonitic micas are increasingly stable at low temperatures (<400°C) at pressures between 4.5 and 0.1 kbar. Similarly, Monier *et al.* (1984) have shown that low-paragonite, high celadonite muscovites reflect low temperatures (<600°C) late to post-magmatic crystallization, which is in excellent agreement with the textural interpretation of the Cairngorm muscovites. Both they and Monier and Robert (1986) have shown that late to post-magmatic muscovites are characterized by low Ti contents, whereas primary muscovites can generally be distinguished by their higher Ti contents (if not simply on textural grounds). Fig. 7 shows that the Cairngorm muscovites lie within the secondary muscovite field of Monier and Robert (1986); their high Fe/Mg ratios reflect those of coexisting biotite.

The origin of the Cairngorm muscovite

The stability of the Cairngorm muscovite lies outside the experimentally determined stability field of Mu + Qtz + Kfspar + Al_2SiO_5 + Vapour as defined by Day (1973) and Chatterjee and Johannes (1974). However, as muscovite is clearly not a phenocryst phase, such a discrepancy is not considered to be unusual.

Burnham (1979) has shown that the crystallization of muscovite from a granitic melt will rapidly become a self-arresting process unless either excess H^+ is present (i.e. a coexisting H_2O-dominated fluid phase), or excess Na and K are removed from the system. If Na and K are not removed from the system then the residual melt will be enriched in alkalis and will move into the crystallization field of K-feldspar. Muscovite crystallization from a melt with an H_2O-dominated fluid phase will be favoured by high water contents (> 9 wt.%), and this essentially pegmatitic style of crystallization will also drive the sericitization reaction into the stability field of muscovite. The

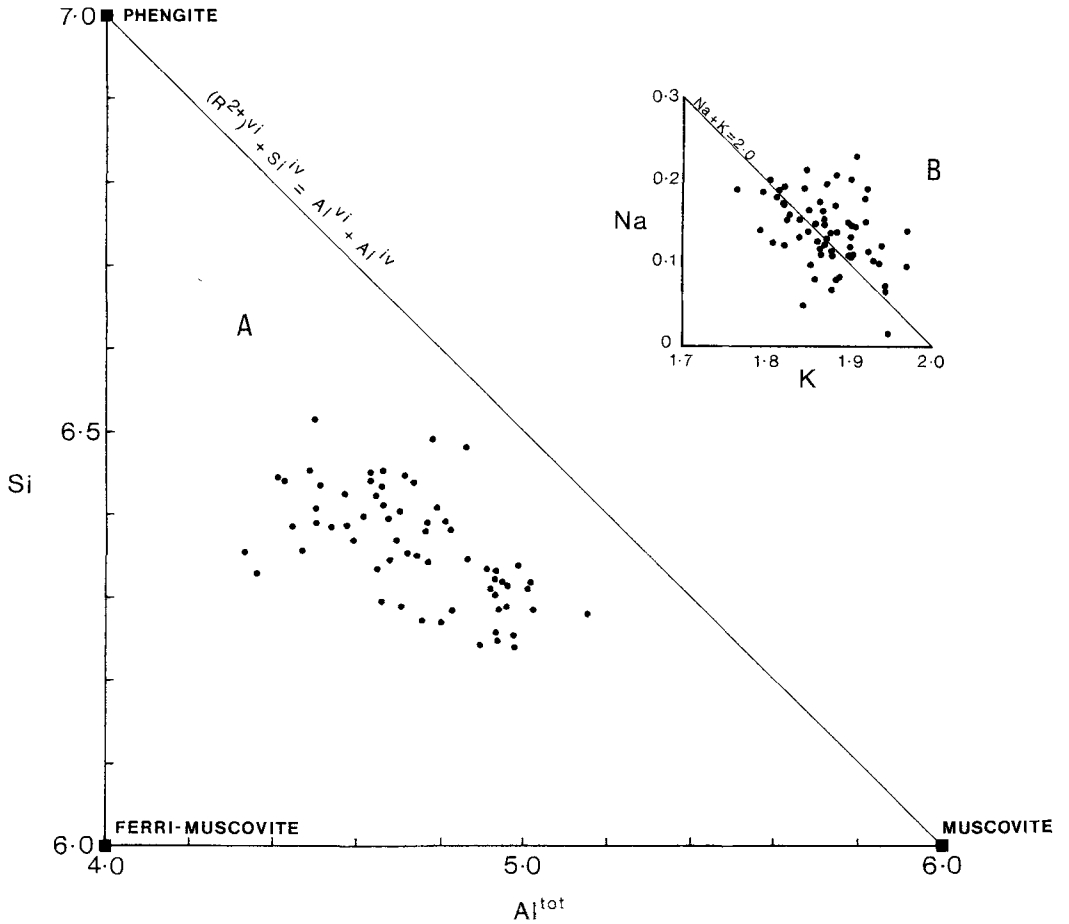

FIG. 6. Composition of Cairngorm muscovite. (A) Si *vs.* Al(tot) showing the relationship to the Al-Tschermak substitution; (B) compositional variation of the interlayer cations.

incomplete reaction of biotite to muscovite in the Cairngorm pluton suggests that the reaction was buffered by the Na + K content of the fluid phase.

Burnham (1979) has also shown that the fluid phase in equilibrium with a granite minimum melt is corundum normative below about 3 kbar. It is concluded that the 'primary looking' Cairngorm muscovites crystallized directly from an Al-saturated fluid-rich residual melt at temperatures largely below the solidus. With the exception of sericite, the remainder of the muscovite has been formed by the breakdown of biotite as it interacted with a late-stage fluid phase, through the reaction

$$\text{Biotite} + \text{fluid} = \text{Phengitic muscovite} + (\text{Fe,Mg,Ti,Mn}) + SiO_2 + K^+.$$

Additional evidence for the crystallization of late muscovite from a fluid-rich residual melt comes from the abundance of large plates of euhedral muscovite in pegmatites within the granite. This residual melt must have been present at temperatures considerably below the solidus since joint surfaces in the granite are locally coated with euhedral muscovite, quartz and K-feldspar.

Fig. 8 shows a limited but well-defined compositional gap between muscovite and biotite, as defined by substitutions (1) and (2). It has been shown earlier that the most aluminous, R^{2+}-poor biotites are those which coexist with muscovite and in which substitution (2) is dominant over (1). However, the reverse is not the case since the most celadonite-rich muscovites have not necessarily formed as an observable alteration product of biotite, suggesting an independent

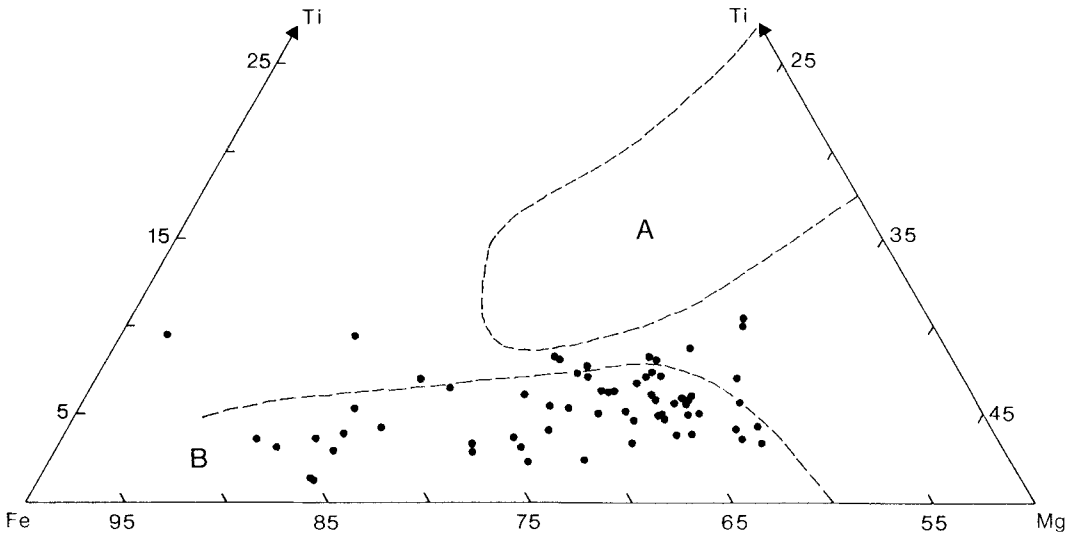

FIG. 7. Composition of Cairngorm muscovite within the fields of primary (A) and secondary (B) muscovite, defined by Monier and Robert (1986).

control for R^{2+} cation distribution in muscovite, probably in response to the buffering of the compositions by the fluid phase.

Discussion

There is no relationship between the degree of alteration and reddening of the feldspars (notably plagioclase) and the R^{2+} contents of the muscovites, despite the potentially very large volumes of R^{2+} cations that can be taken up by the fluid phase during the phengitization of the biotite. Even with a conservative estimate of 5 vol.% biotite and a 2 vol.% muscovite in 1 m^3 of granite, some 23 g of R^{2+} oxide-equivalent is transferred into the fluid phase during phengitization. There is no evidence that such large volumes of material have simply been re-precipitated within the granite.

Field evidence (Harrison, 1987*b*) shows that the pink granite typical of the Cairngorm pluton appears to form a 'cap' some 1000 m thick, below which whiter and less pervasively oxidized granite predominates. Both white and pink granites develop 'primary looking' and secondary muscovite, which suggests that the oxidation of the granite took place after emplacement and is subsolidus.

It seems likely, therefore, that the re-precipitation of a fluid phase rich in R^{2+} cations was facilitated by the fracturing of the pluton roof, possibly during movement on the large strike-slip faults that cut the pluton. The fluids were able to leave via these fracture systems and re-precipitate in hydrothermal systems overlying the pluton. The fracturing of the pluton roof may also have enhanced oxidation through volatile dissociation (Czamanske and Wones, 1973). All faults in the pluton are characterized by infillings of red, cryptocrystalline silica and patches of intensely hematized and silicified granite. Nicholson (1986) has documented Mn and Fe stockwork mineralization adjacent to the Ben Rinnes pluton (35 km to the NE of the Cairngorm pluton) which he attributed to fluid circulation along a fault which cuts the Ben Rinnes pluton. Ben Rinnes is very similar in age, petrography and geochemistry to Cairngorm (Zaleski, 1982; Harrison and Hutchinson, 1987).

Conclusions

Biotite in the Cairngorm pluton displays variable Fe/(Fe + Mg) and Al^{vi} content, whilst Mn increases and Ti decreases with increasing Fe/(Fe + Mg). Increasing Fe/(Fe + Mg) in biotite is controlled largely by dioctahedral–trioctahedral substitutions whereby R^{2+} cations are proxied for Al and an octahedral vacancy. Most of the other compositional variations are controlled by Tschermak-type substitutions.

The compositional variation in the biotite cannot be attributed to simple crystal fractionation processes because the host granite does not show similar chemical variation (e.g. a 3 wt.% range in SiO_2 content). This contrasts with the 'classical' compositional variation in biotite from granitic

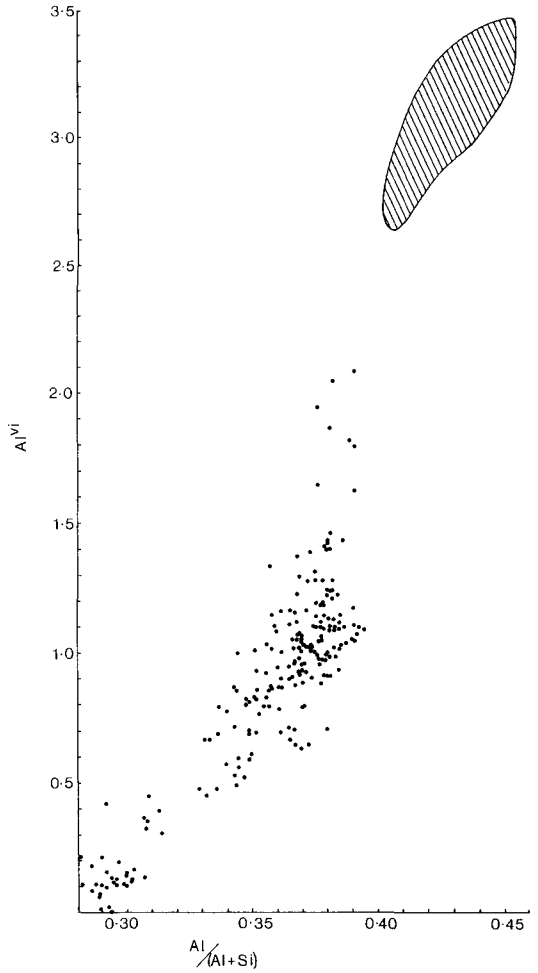

FIG. 8. Al^{vi} *vs.* Al/(Al + Si) (where $Al = Al^{iv} + Al^{vi}$) in Cairngorm biotites, showing the relationship with the compositional field of Cairngorm muscovites (shaded field, containing 64 analyses).

rocks, which generally reflects whole-rock chemical variation (e.g. Czamanske *et al.*, 1981; Dodge *et al.*, 1969; Nockolds and Mitchell, 1946).

Muscovite is locally common in the granite and occurs either as an interstitial primary phase or as an alteration product of biotite. It is phengitic, containing between 15 and 36 mol.% celadonite and <1 mol.% paragonite. Textural evidence and comparison with experimental data suggests that all the muscovites formed at subsolidus temperatures between 500 and 300°C, in response to the extensive but localized development of a peraluminous fluid phase. It is this fluid phase which has also controlled the chemical evolution of the micas—most notably biotite—and has resulted in the formation of unusually Mn- and Al-rich biotite. The fluid phase probably developed at the same time as the oxidation of the granite, and the fracturing of the pluton roof (which may have enhanced oxidation) possibly provided a conduit for the removal of large amounts of R^{2+} cations released from the biotite breakdown and present in solution in the fluid phase.

Acknowledgements

The work was undertaken at Aberdeen University under the tenure of a NERC CASE studentship in conjunction with the British Geological Survey. Microprobe analyses were performed by George Taylor and John Still. The work has benefited from the supervision of Ian Munro, Peter Brown and Doug Fettes, and the helpful guidance of Ian Parsons. The comments of an anonymous referee greatly helped to improve the manuscript. Much of the fieldwork was performed under permit from the Nature Conservancy Council.

References

Albuquerque, C. A. R. de (1973) Geochemistry of biotites from granitic rocks, Northern Portugal. *Geochim. Cosmochim. Acta*, **37**, 1779–802.

Barrière, M. and Cotten, J. (1979) Biotites and associated minerals as markers of magmatic fractionation and deuteric equilibration in granites. *Contrib. Mineral. Petrol.* **70**, 183–92.

Burnham, C. W. (1979) Hydrothermal fluids at the magmatic stage. In *Geochemistry of hydrothermal ore deposits* (2nd ed.) (Barnes, H. L., ed.), 34–76.

Chatterjee, N. D. and Johannes, W. (1974) Thermal stability and thermodynamic properties of synthetic $2M_1$ muscovite, $KAl_2(AlSi_3)O_{10}(OH)_2$. *Contrib. Mineral. Petrol.* **48**, 89–114.

Czamanske, G. K. and Wones, D. R. (1973) Oxidation during magmatic differentiation, Finnmarka complex, Oslo area, Norway: Part 2, the mafic silicates. *J. Petrol.* **14**, 349–80.

—— Ishihara, S. and Atkin, S. A. (1981) Chemistry of rock-forming minerals of the Cretaceous–Palaeocene batholith in southwestern Japan and implications for magma genesis. *J. Geophys. Res.* **86**, 10431–69.

Day, H. W. (1973) High-temperature stability of muscovite plus quartz. *Am. Mineral.* **58**, 255–62.

Dodge, F. C. W., Smith, V. C. and Mays, R. E. (1969) Biotites from the granitic rocks of the Sierra Nevada Batholith, California. *J. Petrol.* **10**, 250–71.

Dymek, R. F. (1983) Titanium, aluminium and interlayer cation substitutions in biotite from high-grade gneisses, west Greenland. *Am. Mineral.* **68**, 880–99.

Fenn, P. M. (1986) On the origin of graphic granite. Ibid. **71**, 325–30.

Foster, M. D. (1960) Layer charge relations in the dioctahedral and trioctahedral micas. Ibid. **45**, 383–98.

Harrison, T. N. (1987*a*) The mode of emplacement of the Cairngorm granite. *Scott. J. Geol.* **22**, 303–14.

—— (1987*b*) *The evolution of the Eastern Grampians*

granitoids. Unpubl. Ph.D. thesis, University of Aberdeen.

—— (1988) Magmatic garnets in the Cairngorm granite, Scotland. *Mineral. Mag.* **52,** 659–67.

—— and Hutchinson, J. (1987) The age and origin of the Eastern Grampians Newer Granites. *Scott. J. Geol.* **23,** 269–82.

Hazen, R. M. and Wones, D. R. (1972) Predicted and observed compositional limits of trioctahedral micas. *Am. Mineral.* **63,** 885–92.

Hewitt, D. A. and Abrecht, J. (1986) Limitations on the interpretation of biotite substitutions from chemical analyses of natural samples. Ibid. **71,** 1126–8.

Hewitt, D. A. and Wones, D. R. (1975) Physical properties of some synthetic Fe-Mg-Al trioctahedral micas. Ibid. **60,** 854–62.

Labotka, T. C. (1983) Analysis of compositional variations of biotite in pelitic hornfelses from northeastern Minnesota. Ibid. **68,** 900–14.

Leroy, J. and Cathelineau, M. (1982) Les minéraux phylliteaux dans les gisements hydrothermaux d'uranium. I. Cristallochimie des micas hérités et néoformés. *Bull. Minéral.* **105,** 99–109.

Mahood, G. and Hildreth, W. (1983) Large partition coefficients for trace elements in high-silica rhyolites. *Geochim. Cosmochim. Acta*, **47,** 11–30.

Miller, C. F., Stoddard, E. F., Bradfish, L. J. and Dollase, W. A. (1981) Composition of plutonic muscovite: genetic implications. *Can. Mineral.* **19,** 25–34.

Monier, G. (1987) Cristallochimie des micas des leucogranites. Nouvelles données experimentales et applications pétrologiques. *Geol. Geochim. Uranium (Nancy)*, **14.**

—— and Robert, J.-L. (1986) Titanium in muscovites from two-mica granites: substitutional mechanism and partition with coexisting biotites. *Neues Jahrb. Mineral. Abh.* **153,** 147–61.

—— Mergoil-Daniel, J. and Labernardière, H. (1984) Generations successives de muscovites et feldspaths potassiques dans les leucogranites du Millevaches (Massif Central français). *Bull. Minéral.* **107,** 55–68.

Nicholson, K. (1986) Mineralogy and geochemistry of manganese and iron veins, Arndilly, Banffshire. *Scott. J. Geol.* **23,** 213–24.

Nockolds, S. R. and Mitchell, R. L. (1946) The geochemistry of some Caledonian plutonic rocks: a study in the relationship between major and trace elements of igneous rocks and their minerals. *Trans. R. Soc. Edinb.* **61,** 533–75.

Robert, J.-L. (1976) Titanium solubility in synthetic phlogopite solid solutions. *Chem. Geol.* **17,** 213–27.

Streckeisen, A. L. (1976) To each plutonic rock its proper name. *Earth Sci. Rev.* **12,** 1–33.

Thompson, J. B. Jr. (1982) Compositional space: an algebraic and geometric approach. In *Characterization of metamorphism through mineral equilibria* (Ferry, J. M., ed.) *Reviews in Mineralogy*, **10,** 1–32.

Velde, B. (1965) Phengite micas: synthesis, stability and natural occurrence. *Am. J. Sci.* **263,** 886–913.

—— (1972) Celadonite mica: solid solution and stability. *Contrib. Mineral. Petrol.* **37,** 235–47.

Whittaker, E. J. W. and Muntus, R. (1970) Ionic radii for use in geochemistry. *Geochim. Cosmochim. Acta*, **34,** 945–56.

Zaleski, E. (1982) *The geology of Speyside and lower Findhorn granitoids*. Unpubl. M.Sc. thesis, University of St. Andrews.

[*Manuscript received 24 July 1989; revised 26 September 1989*]